



High-Temperature Kinetics of AlCl_3 Decomposition in the Presence of Additives for Chemical Vapor Deposition

Laurent Catoire^{a,*} and Mark T. Swihart^{b,*}

^aLaboratoire de Combustion et Systèmes Réactifs-Centre National de la Recherche Scientifique and University of Orleans, F-45071 Orleans Cedex 2, France

^bDepartment of Chemical Engineering, The State University of New York at Buffalo, Buffalo, New York 14230-4200 USA

A numerical study has been performed modeling the gas-phase reactions occurring during the chemical vapor deposition (CVD) of alumina from $\text{AlCl}_3/\text{CO}_2/\text{H}_2$ mixtures. The purpose is to answer whether and to what extent trends in the decomposition of AlCl_3 via gas-phase reactions can explain experimentally observed trends in CVD deposition of aluminum-containing films. The AlCl_3 decomposition is predicted to occur via a free-radical chain mechanism that, in the presence of H_2 , has H atoms and the AlCl_2 radical as the primary chain carriers. We find that the present kinetic model predicts trends for the decomposition rate of AlCl_3 in the gas phase that are consistent with trends observed experimentally for the Al_2O_3 deposition rate. Based on these results, the chemical kinetics model is used to study the effects on AlCl_3 thermal decomposition of other additives (H_2O_2 , H_2O , O_2 , Cl_2) for which no experimental data are available in the literature. H_2O_2 is predicted to be a particularly efficient promoter for AlCl_3 thermal decomposition. The mechanism also predicts that the presence of AlCl_3 dramatically increases the rate of H_2O production compared to H_2O production from CO_2 and H_2 in the absence of AlCl_3 .
© 2002 The Electrochemical Society. [DOI: 10.1149/1.1467366] All rights reserved.

Manuscript received May 23, 2001. Available electronically April 2, 2002.

Aluminum trichloride (AlCl_3) is a popular Al-containing precursor for the gas-phase combustion synthesis of particles and for chemical vapor deposition (CVD) of films and coatings. Depending on the material to be deposited, several gas mixtures have been considered. The CVD of alumina (Al_2O_3) has been realized with various mixtures, but most frequently using $\text{AlCl}_3/\text{CO}_2/\text{H}_2$ mixtures as presented by Lux and Schachner,¹ Colmet *et al.*,² Colombier *et al.*,³ Bae *et al.*,⁴ and others. Recently, Schierling *et al.*⁵ used the $\text{AlCl}_3/\text{CO}_2/\text{H}_2/\text{HCl}$ mixtures for the deposition of alumina, and Nitodas and Sotirchos⁶ studied the codeposition of alumina and silica using $\text{AlCl}_3/\text{SiCl}_4/\text{H}_2/\text{CO}_2$ mixtures and $\text{CH}_3\text{SiCl}_3/\text{AlCl}_3/\text{CO}_2/\text{H}_2$ mixtures.⁷

Although various effects of reactor conditions on the deposition kinetics of alumina have been observed and reported in the above-cited works and references therein, the fundamental gas-phase and surface chemistry occurring in these systems remains largely unstudied. This is not surprising, since, on one hand, there is a lack of thermochemical and elementary kinetic data for reactions in this system and, on the other hand, the overall deposition process involves many homogeneous and heterogeneous reactions; it is not obvious which of these reactions control material growth rates and properties.

The aim of this paper is to study numerically the thermal decomposition of AlCl_3 in the presence of various gaseous additives (H_2 , HCl , CO_2) at conditions (composition, temperature, and pressure) of interest for CVD of alumina. In the present study, we confine our investigation to gas-phase chemistry only, though surface reactions are obviously also important and will be the topic of future studies. Rate parameters for a large number of gas-phase reactions have been computed or estimated based on *ab initio* quantum chemical calculations using transition state theory (TST) and unimolecular rate theories. For reactions not studied by *ab initio* methods, semi-empirical techniques have been used to estimate rate parameters. This has allowed the construction of a detailed gas-phase reaction mechanism for this system and its use to simulate AlCl_3 decomposition as described above.

Reaction Mechanism and Thermochemistry

Due to space limitations, it is not possible to list the complete reaction mechanism, but it can be obtained from the authors upon request. This mechanism consists of 104 reversible chemical reactions among 35 species. It is based on an Al/HCl submechanism proposed by Swihart *et al.*,^{8,9} primarily devoted to the combustion of aluminum particles in HCl, and relevant reactions from the less well-understood Al/C/O/Cl/H system. Some possible reactions are not included in the model, due to the lack of kinetic data and information on whether they can even occur, and this model cannot be considered as final. In particular, pathways for the gaseous formation of alumina and nucleation of alumina particles are not included in detail. However, since the surface reactions are also not considered here, our goal here is not to examine the deposition rate of alumina in terms of alumina formation, but in terms of AlCl_3 decomposition rate. The question we attempt to answer here is whether and to what extent trends in the decomposition of AlCl_3 via gas-phase reactions can explain experimentally observed trends in CVD deposition of aluminum-containing films from it.

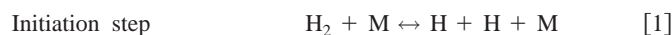
The CHEMKIN-II¹⁰ and SENKIN¹¹ codes were used to integrate the time dependent rate equations derived from the reaction mechanism for a well-mixed, batch reactor. The thermodynamic properties for the Al-containing species have been calculated using *ab initio* quantum chemical methods.¹² All the data for the non-Al-containing species have been taken from the CHEMKIN-II Library¹³ or from the thermochemical tables of Burcat and McBride.¹⁴

Experimental Trends Rationalized by this Kinetic Model

Effect of the partial pressure of H_2 .—Hydrogen plays an important role as it enhances the deposition rate of Al_2O_3 from $\text{AlCl}_3\text{-CO}_2$ mixtures. The trends observed for the alumina deposition are expected to follow the trends predicted for AlCl_3 decomposition. This enhancing effect of H_2 is predicted by the kinetic model under consideration, as shown in Fig. 1. For the mixture 2 mbar AlCl_3 + 2 mbar CO_2 + 96 mbar Ar at 1323 K, AlCl_3 decomposes very little for times up to 4 s. For the mixture 2 mbar AlCl_3 + 2 mbar CO_2 + 96 mbar H_2 at 1323 K, AlCl_3 decomposes more significantly. Local sensitivity analyses show that several reactions are responsible for the enhancing effect observed. Reaction sequences involved are

* Electrochemical Society Active Member.

[†] E-mail: catoire@cns-orleans.fr



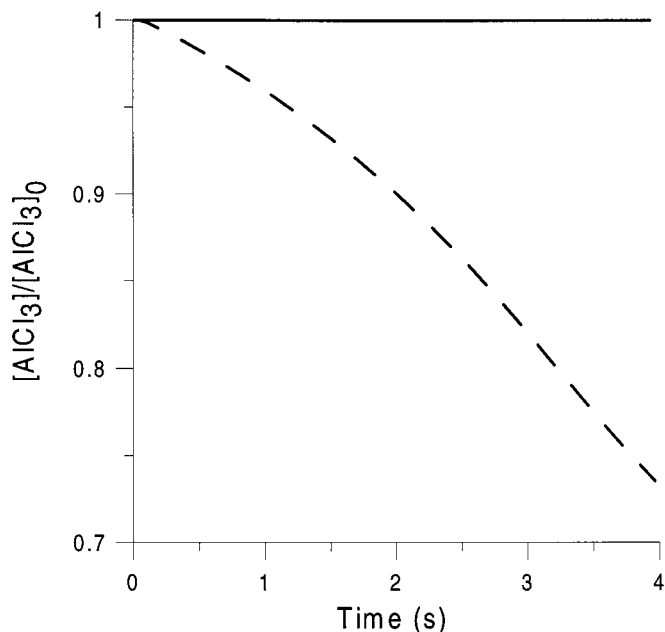
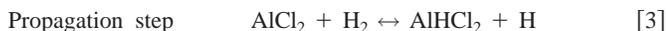
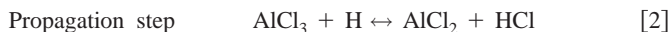


Figure 1. Calculated AlCl_3 profiles for the mixture 2 mol % AlCl_3 + 2 mol % CO_2 in Ar (full line) and for the mixture 2 mol % AlCl_3 + 2 mol % CO_2 in H_2 (dashed line). Total pressure for both mixtures is 100 mbar and the temperature is 1323 K.



together with



The influence of the H_2 partial pressure on the Al_2O_3 deposition rate from $\text{AlCl}_3/\text{CO}_2/\text{H}_2$ mixtures has been experimentally shown by Schierling *et al.*⁵ for five different mixtures (see Fig. 9 in Ref. 5). Increasing the H_2 partial pressure in the feed gas increases the deposition rate. The kinetic model predicts that the rate of decomposition of AlCl_3 is increased by increasing H_2 partial pressure as shown in Fig. 2 and 3 for two of the Schierling *et al.* experimental mixtures, one at 100 mbar total pressure, and the other at 1000 mbar total pressure.

Effect of the partial pressure of HCl.—Schierling *et al.*,⁵ among others, show that increasing HCl partial pressure leads to a decrease in the Al_2O_3 deposition rate (see Fig. 2 in Ref. 5). The present model predicts that the AlCl_3 decomposition rate decreases if a significant amount of HCl is present in the mixture as shown in Fig. 4. A sensitivity analysis shows that HCl inhibits the AlCl_3 thermal decomposition by reacting with AlCl_2 according to $\text{AlCl}_2 + \text{HCl} \leftrightarrow \text{AlCl}_3 + \text{H}$, *i.e.*, AlCl_3 is reformed by the reverse of Reaction 2 listed above. The inhibitory effect of HCl only becomes apparent at relatively large concentrations of HCl, since these large concentrations are required to significantly shift the equilibrium of Reaction 2.

Effect of the partial pressure of AlCl_3 .—The rate of alumina deposition is reported to rise with the AlCl_3 partial pressure but to become constant above a certain AlCl_3 pressure.⁵ The reaction orders with respect to AlCl_3 were between 2 and 0.⁵ Figure 5 shows that the AlCl_3 decomposition rate increases as AlCl_3 partial pressure

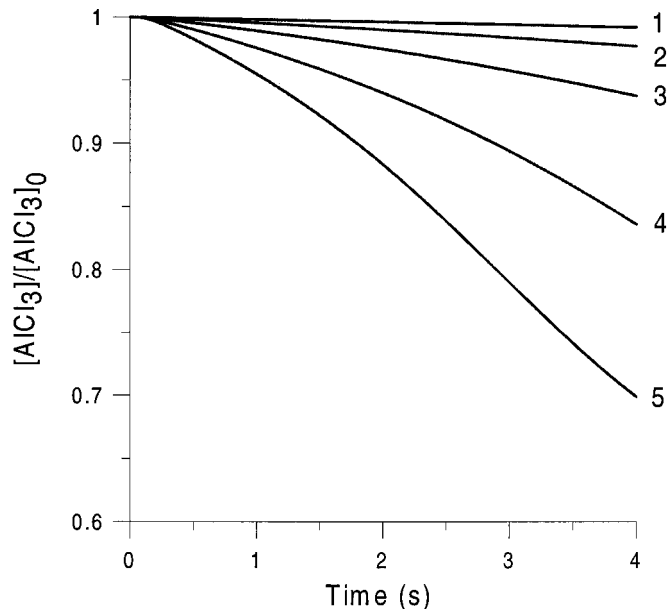


Figure 2. Calculated AlCl_3 profiles at total pressure of 100 mbar and at 1323 K for the mixtures: (1) 0.1 mol % HCl + 1 mol % AlCl_3 + 0.6 mol % CO_2 + 2 mol % H_2 in Ar; (2) HCl, AlCl_3 , and CO_2 as in 1 + 7 mol % H_2 in Ar; (3) HCl, AlCl_3 , and CO_2 as in 1 + 20 mol % H_2 in Ar; (4) HCl, AlCl_3 , and CO_2 as in 1 + 50 mol % H_2 in Ar; and (5) HCl, AlCl_3 , and CO_2 as in 1 in H_2 .

increases. In fact, the situation appears complex as the apparent reaction order evolves with time. However, the fact that the deposition rate increases as AlCl_3 partial pressure increases can be explained based on occurrences in the gas phase. Note that if AlCl_3 decomposition were first order, all four curves in Fig. 5 would be the same. Thus, the reaction rate is more than first order in AlCl_3 at

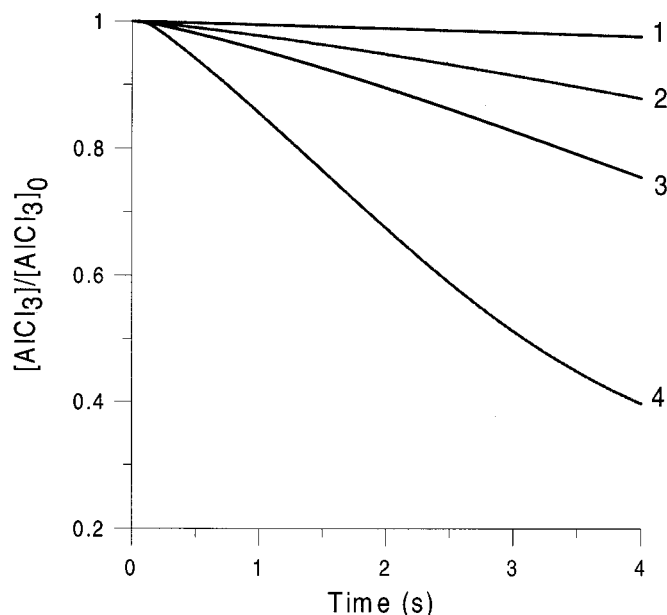


Figure 3. Calculated AlCl_3 profiles at total pressure of 1000 mbar and at 1323 K for the mixtures: (1) 0.8 mbar HCl + 0.8 mbar AlCl_3 + 5.2 mbar CO_2 + 6 mbar H_2 in Ar; (2) HCl, AlCl_3 , and CO_2 as in 1 + 40 mbar H_2 in Ar; (3) HCl, AlCl_3 , and CO_2 as in 1 + 90 mbar H_2 in Ar; and (4) HCl, AlCl_3 , and CO_2 as in 1 + 384 mbar H_2 in Ar.

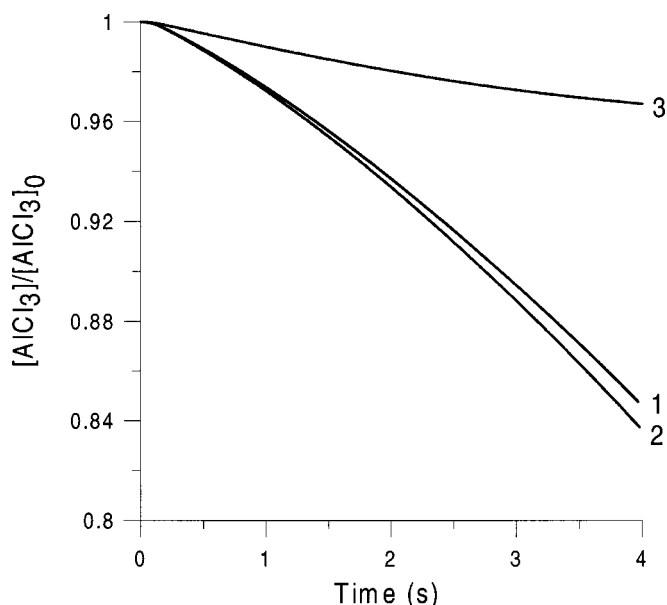


Figure 4. Calculated AlCl_3 profiles at total pressure of 100 mbar and at 1323 K for the mixtures: (1) 0.06 mbar HCl + 1.3 mbar AlCl_3 + 4 mbar CO_2 + 60 mbar H_2 in Ar; (2) H_2 , AlCl_3 , and CO_2 as in 1 + 0.5 mbar HCl in Ar; and (3) H_2 , AlCl_3 , and CO_2 as in 1 + 26 mbar HCl in Ar.

short times and at low AlCl_3 concentrations, but less than first order in AlCl_3 at higher AlCl_3 concentrations and at longer times.

Effect of the partial pressure of CO_2 .—Schierling *et al.*⁵ observed that increasing the CO_2 partial pressure increases the Al_2O_3 deposition rate. Nitodas and Sotirchos⁶ show that, depending on the values of the other operating parameters, an increase in the CO_2 mole fraction may increase, decrease, or have no effect on the depo-

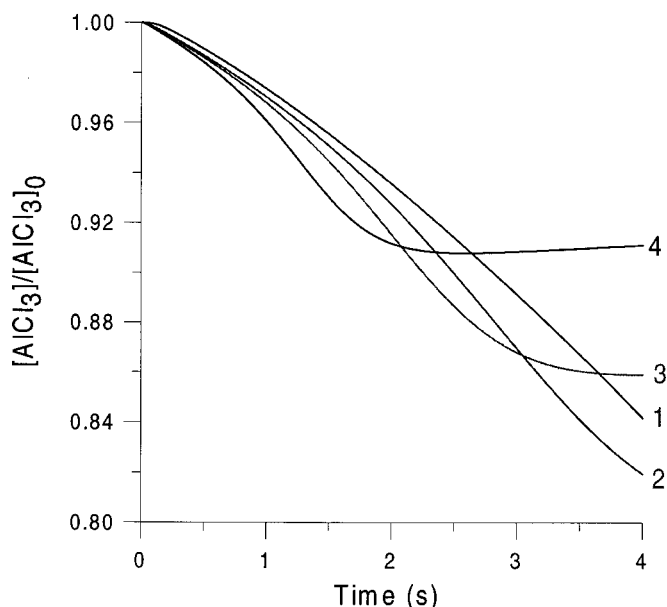


Figure 5. Calculated AlCl_3 profiles at total pressure of 100 mbar and at 1323 K for the mixtures: (1) 0.3 mbar HCl + 1 mbar AlCl_3 + 4 mbar CO_2 + 60 mbar H_2 in Ar; (2) 0.3 mbar HCl + 5 mbar AlCl_3 + 4 mbar CO_2 + 60 mbar H_2 in Ar; (3) 0.3 mbar HCl + 9 mbar AlCl_3 + 4 mbar CO_2 + 60 mbar H_2 in Ar; and (4) 0.3 mbar HCl + 18.7 mbar AlCl_3 + 4 mbar CO_2 + 60 mbar H_2 in Ar.

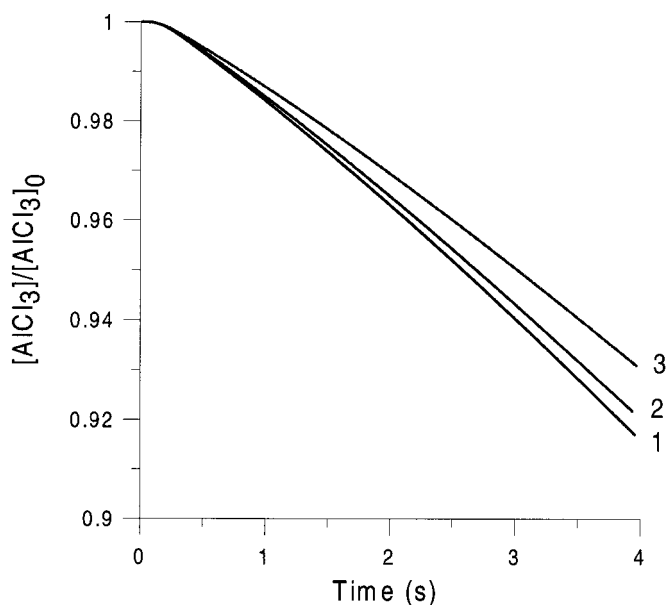


Figure 6. Calculated AlCl_3 profiles at total pressure of 100 torr and at 1273 K for the mixtures: (1) 1.2 mol % AlCl_3 + 3.5 mol % CO_2 in H_2 ; (2) 1.2 mol % AlCl_3 + 10 mol % CO_2 in H_2 ; and (3) 1.2 mol % AlCl_3 + 24 mol % CO_2 in H_2 .

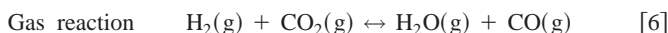
sition rate. Figure 6 shows that the AlCl_3 decomposition rate is not strongly influenced by the CO_2 mole fraction. However, for the corresponding Al_2O_3 deposition rate reported by Nitodas and Sotirchos (see Fig. 6 in Ref. 6), the promoting effect of the CO_2 partial pressure on the alumina deposition rate was relatively weak. In that case, an increase by a factor of 6.6 (up to 24 mol %) in the partial pressure of CO_2 led to an increase in the alumina deposition rate by only a factor of 1.5. One can also interpret this result as indicating that the effect of CO_2 concentration on alumina deposition is not due to reactions in the gas phase, or that it is due to gas-phase processes, such as the rate of H_2O production, that are not directly reflected by the rate of AlCl_3 decomposition.

Effect of the temperature.—Experimentally, an increase in temperature increases the Al_2O_3 deposition rate. Figure 7 shows that, as expected, an increase in temperature also increases the predicted AlCl_3 decomposition rate.

Summary of Gas-Phase $\text{AlCl}_3/\text{CO}_2/\text{H}_2/\text{HCl}$ Chemistry

Schierling *et al.* in their recent publication recognized that the details of the gas-phase chemistry in this system remain to be investigated.⁵ Based on the consistency of the present model with a variety of experimental observations, we now apply this model to attempt to understand what happens in the gas phase.

It has been widely proposed that the CVD of alumina from $\text{AlCl}_3/\text{H}_2/\text{CO}_2$ mixtures follows the following overall equations



Nevertheless, the present kinetic model predicts that at the temperature of about 1300-1350 K, the H_2/CO_2 reaction, in the absence of AlCl_3 , does not produce water in significant amounts even after very long reaction times of several tens of seconds. In fact, gas-phase formation of significant amounts of water in a reasonable reactor residence time at these temperatures requires the presence of AlCl_3 , as shown in Fig. 8. Therefore, the kinetics in the gas phase are not as simple as those of the single Reaction 6 above, and we consider them in more detail here.

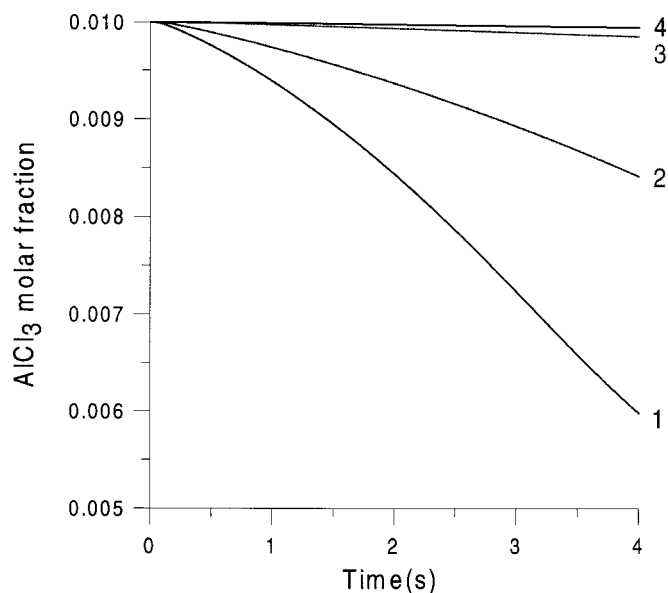


Figure 7. Calculated AlCl_3 profiles at total pressure of 100 mbar for the mixture 0.1 mol % HCl + 1 mol % AlCl_3 + 2 mol % CO_2 + 60 mol % H_2 in Ar at (1) 1359 K, (2) 1323 K, (3) 1228 K, and (4) 1187 K.

Local sensitivity analyses have been performed for all the species for the representative mixture 0.8 mbar AlCl_3 + 0.8 mbar HCl + 5.2 mbar CO_2 + 384 mbar H_2 in Ar (see Schierling *et al.*⁵) at 1000 mbar total pressure and 1323 K. These sensitivity analyses show that AlCl_3 disappears principally through Reaction 2. The H atoms being initially produced by the Reaction 1 (see Fig. 9), and later by Reaction 3 and



Note that Reaction 8 serves as a chain branching step in the free-radical decomposition of AlCl_3 , since it converts a molecular product of a propagation step (AlHCl_2) into two free-radical chain carriers (AlCl_2 and H).

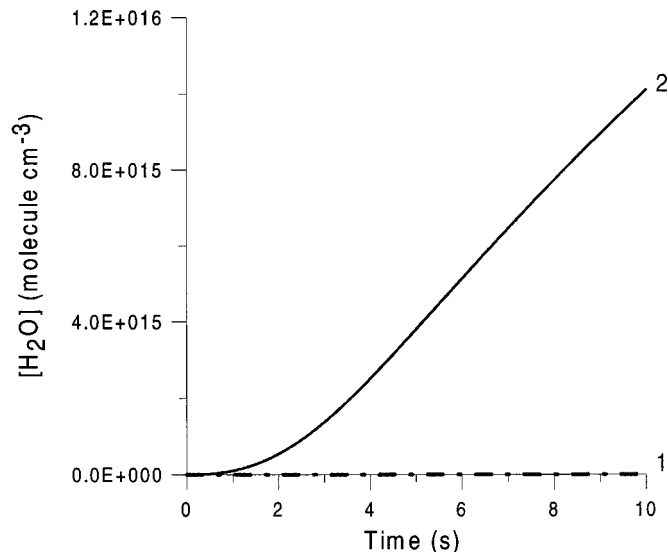


Figure 8. H_2O profile formed in the mixture at 1000 mbar total pressure and 1323 K: (1) 5.2 mbar CO_2 + 384 mbar H_2 in Ar, and (2) 5.2 mbar CO_2 + 384 mbar H_2 + 0.8 mbar AlCl_3 + 0.8 mbar HCl in Ar (mixture from Ref. 5).

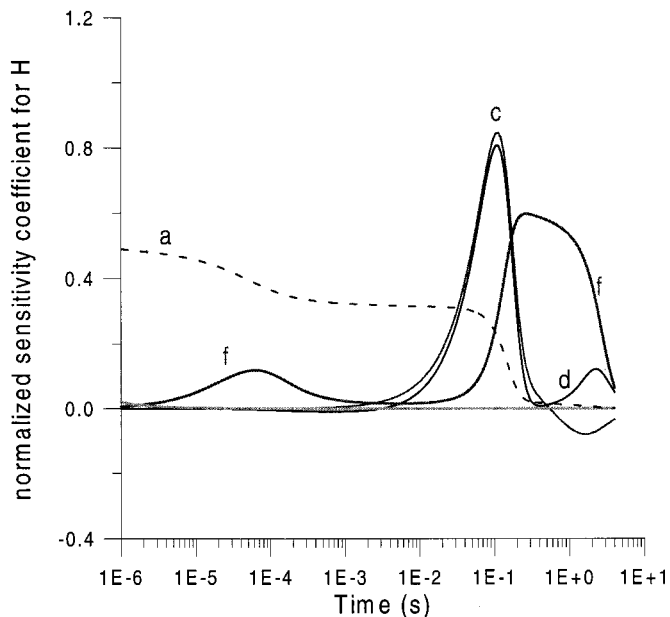


Figure 9. Sensitivity plot for H: (a) $\text{H}_2 (+\text{M}) \leftrightarrow \text{H} + \text{H} (+\text{M})$, (c) $\text{AlHCl}_2 \leftrightarrow \text{AlCl}_2 + \text{H}$, (d) $\text{AlCl}_3 + \text{H} \leftrightarrow \text{AlCl}_2 + \text{HCl}$, and (f) $\text{AlHCl}_2 + \text{H} \leftrightarrow \text{AlCl}_2 + \text{H}_2$.

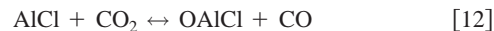
Water formation is predicted to occur primarily by the reaction



AlO is formed by the reactions (see Fig. 10)



OAlCl is mostly formed by



AlCl is formed by the sequence Reaction 3 followed by



The formation of water is potentially of importance as it is generally believed that alumina is formed through the global surface Reaction 7. As stated above, the present work predicts that water is formed primarily via Reaction 9, and the reaction sequence



followed by



(globally the water shift reaction) appears to be unimportant. Its removal from the kinetic model does not appreciably change the computed water concentration profiles.

It is known that the reverse of Reaction 14 ($\text{CO} + \text{OH} \rightarrow \text{CO}_2 + \text{H}$) occurs as a chemically activated reaction, and exhibits pressure dependence. Therefore, we initially used a Lindemann treatment of this pressure dependence with the rate constants k_∞ (high-pressure limiting rate constant) and k_0 (low-pressure limiting rate constant) calculated by Larson *et al.*¹⁵ However, above 1090 K in the pressure range 0.19-0.82 atm, Wooldridge *et al.*¹⁶ did not observe any measurable pressure dependence and proposed a pressure-independent rate constant k ($\text{cm}^3 \text{mol}^{-1} \text{s}^{-1}$) = $2.12 \times 10^{12} \exp(-2630/T)$ for this reaction. Wooldridge *et al.* also

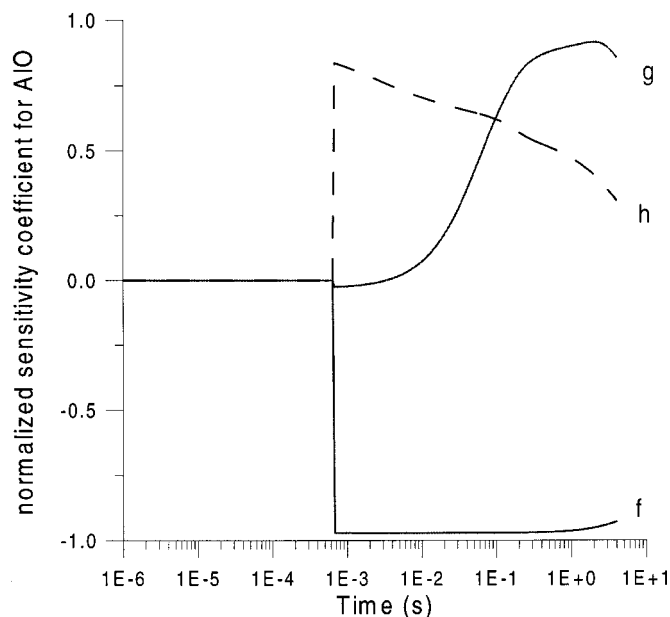


Figure 10. Sensitivity plot for AlO: (f) $\text{Al} + \text{H}_2\text{O} \leftrightarrow \text{AlO} + \text{H}_2$, (g) $\text{AlO} + \text{HCl} \leftrightarrow \text{OAlCl} + \text{H}$, and (h) $\text{Al} + \text{CO}_2 \leftrightarrow \text{AlO} + \text{CO}$.

showed good agreement of their experiments with the treatment followed by Larson *et al.*¹⁵ The use of the rate constant of Wooldridge *et al.*¹⁶ slightly extrapolated to 1 bar in the kinetic model leads to the conclusion that water is formed competitively through the reaction sequence given above (Reactions 9-13), and the following sequence of Reactions 14 and 15 followed by



However, removal of Reaction 15 from the kinetic model leads only to a slightly decrease in water production, and it appears that the water/gas shift reaction is not necessary to explain the formation of water. In fact, only the simultaneous removal of Reactions 9, 15, and 16 is able to dramatically decrease the predicted formation of water. Each channel on its own is able to form water in comparable amounts, and therefore the three channels are not only competitive but coupled. Note that even when water formation via Reaction 9, which directly involves an aluminum containing species, is eliminated, AlCl_3 still accelerates water formation. This is because AlCl_3 serves as a source of the H radicals that participate in Reaction 14 above, via the reaction sequence Reaction 4 followed by Reaction 5.

Effect of Additives Not Studied Experimentally

This chemical kinetic model has also been used to predict of the effect of additives that have not been studied experimentally, including O_2 , Cl_2 , H_2O , H_2O_2 . However, this effect only concerns the gas phase and nothing can be said here about the ability of such mixtures to form alumina with the appropriate properties (impurity content, powder size and morphology, film morphology, etc.). It is of interest to search for additives able to increase the deposition rate of alumina, which is, in many of the experiments presented in the literature, relatively slow.

Effect of the partial pressure of Cl_2 .— Cl_2 is predicted to be an inhibitor of the AlCl_3 thermal decomposition, just as HCl is, when present in significant amounts. Moreover, as shown in Fig. 11, Cl_2 has a stronger inhibiting effect than HCl (at least for the conditions considered here).

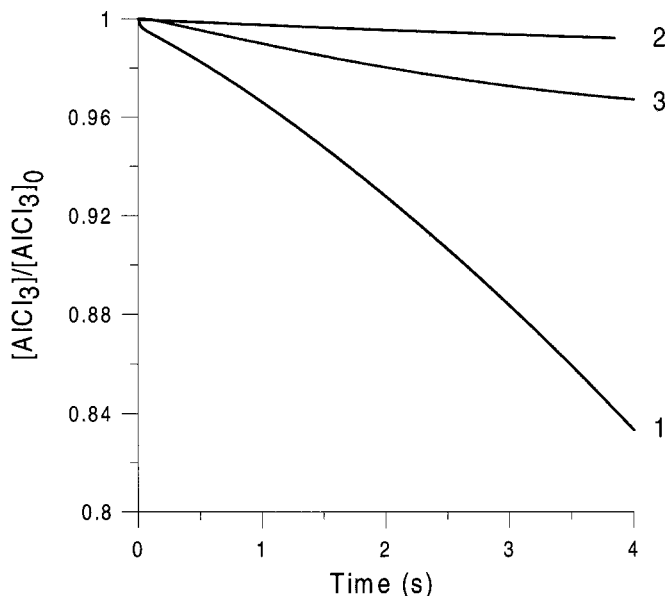


Figure 11. Calculated AlCl_3 profiles at total pressure of 100 mbar and at 1323 K for the mixtures: (1) 0.06 mbar Cl_2 + 1.3 mbar AlCl_3 + 4 mbar CO_2 + 60 mbar H_2 in Ar; (2) H_2 , AlCl_3 , and CO_2 as in 1 + 26 mbar Cl_2 in Ar; and (3) H_2 , AlCl_3 , and CO_2 as in 1 + 26 mbar HCl in Ar.

Effect of the partial pressure of water.—Water is predicted to have no significant effect on the thermal decomposition rate of AlCl_3 under CVD conditions, even when present in significant quantities, as shown in Fig. 12.

Effect of the partial pressure of hydrogen peroxide.—Hydrogen peroxide (H_2O_2) is predicted to be a promoter for AlCl_3 thermal decomposition even at very low levels as shown in Fig. 13 and 14. With significant amount of H_2O_2 in the mixture, the AlCl_3 decomposition rate is dramatically increased as shown in Fig. 13 and 14. The explanation of this promoting effect is given by the reaction sequence



followed by Reaction 15 that serves as a source of H atoms for reaction with AlCl_3 . However, the conditions of mixture 3 of Fig. 14 are not realistic ones for CVD processes, as this mixture is predicted by this kinetic model to lead, under adiabatic conditions, to ignition almost instantaneously (ignition delay time of about 7 μs , constant-volume flame temperature of about 2640 K). This is relevant to the flame particle synthesis process, but not to conventional CVD. In contrast, mixture 2 is predicted to react under about isothermal and isobaric conditions due to the low level of hydrogen peroxide present in the mixture (0.06 mol %). This promoting effect of hydrogen peroxide can, therefore, be of potential use in the CVD process to increase deposition rates. However, as underlined above, these kinetics considerations only concern the gas phase, and the predicted promoting effect of hydrogen peroxide has to be experimentally demonstrated. Experimentally, adding H_2O_2 to this deposition system would introduce substantial new safety concerns, due to the possibility of forming explosive mixtures. In this regard, detailed chemical kinetic models like the one used here can be of use in identifying explosion limits, allowing experiments to be conducted outside of them.

Effect of the partial pressure of CO.—Strictly speaking, CO has been studied as an additive for the kinetics of alumina deposition from $\text{AlCl}_3/\text{CO}_2/\text{H}_2$ mixtures, but the compositions of the mixtures studied are not given in the literature. A retarding effect of CO is reported by Lux and Schachner¹ whereas, according to Schierling

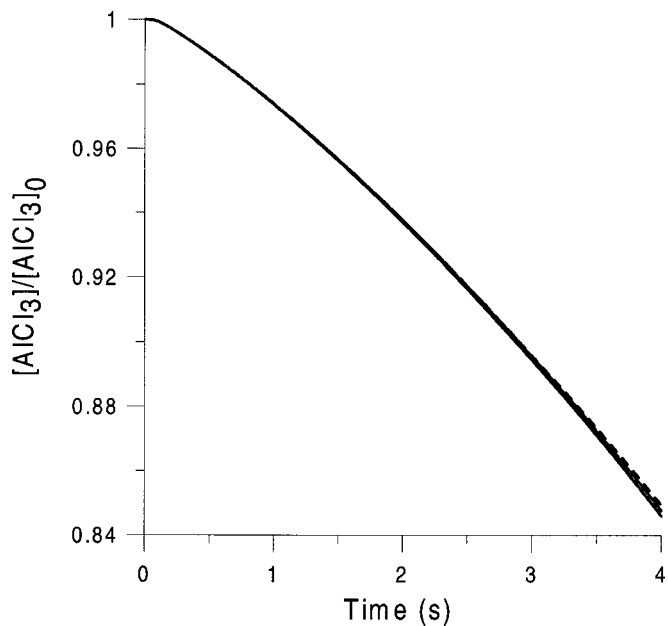


Figure 12. Calculated AlCl₃ profiles at total pressure of 100 mbar and at 1323 K for the mixtures: (—) 0.06 mbar HCl + 1.3 mbar AlCl₃ + 4 mbar CO₂ + 60 mbar H₂ in Ar; (---) H₂, AlCl₃, and CO₂ as in 1 + 0.06 mbar H₂O in Ar (H₂O has replaced HCl in the mixture), and (—) H₂, AlCl₃, and CO₂ as in 1 + 26 mbar H₂O in Ar.

et al.,⁵ CO has no effect in the pressure range tested (1 to 14 mbar, but the partial pressures of the other constituents are not given). Here, we have considered only one mixture, and in this case, CO is predicted to have no effect at low levels and to be a promoter when present in significant amounts as shown in Fig. 15. As was the case for CO₂, the role of CO has to be clarified further.

Effect of the partial pressure of O₂.—O₂ is predicted to be a

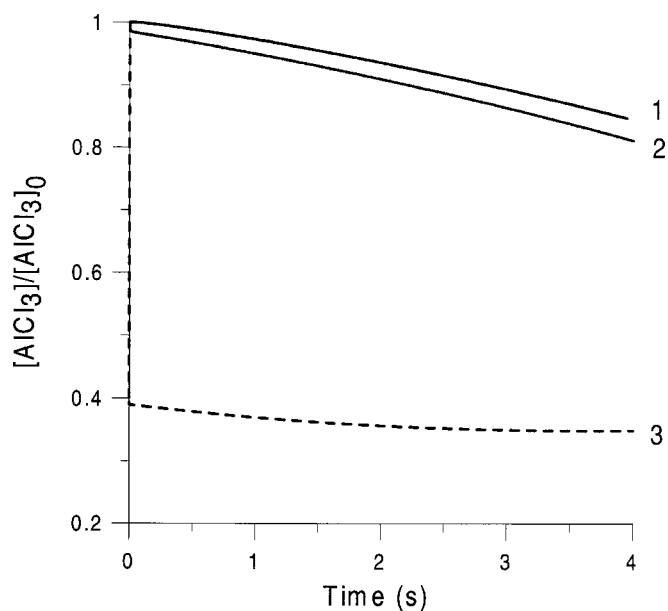


Figure 13. Calculated AlCl₃ profiles at total pressure of 100 mbar and at 1323 K for the mixtures: (1) 0.06 mbar HCl + 1.3 mbar AlCl₃ + 4 mbar CO₂ + 60 mbar H₂ in Ar; (2) H₂, AlCl₃, and CO₂ as in 1 + 0.06 mbar H₂O in Ar; and (3) H₂, AlCl₃, and CO₂ as in 1 + 26 mbar H₂O₂ in Ar.

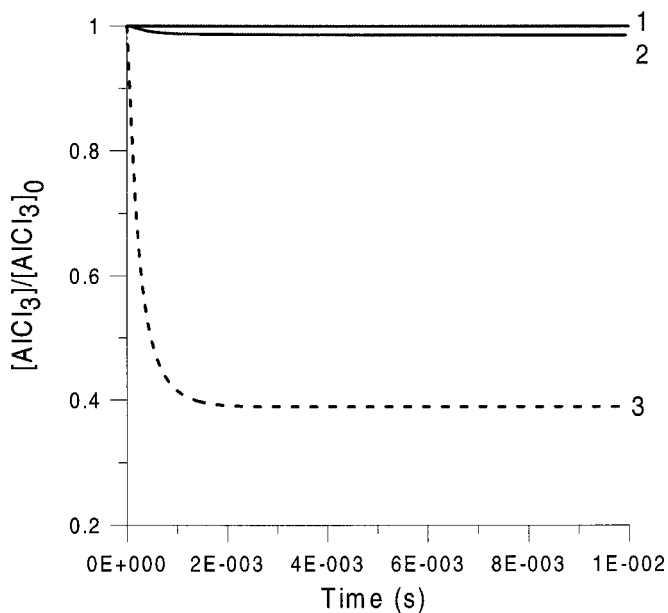


Figure 14. Calculated AlCl₃ profiles at total pressure of 100 mbar and at 1323 K for the mixtures: (1) 0.06 mbar HCl + 1.3 mbar AlCl₃ + 4 mbar CO₂ + 60 mbar H₂ in Ar; (2) H₂, AlCl₃, and CO₂ as in 1 + 0.06 mbar H₂O₂ in Ar; and (3) H₂, AlCl₃, and CO₂ as in 1 + 26 mbar H₂O₂ in Ar.

promoter for AlCl₃ thermal decomposition even at very low levels as shown in Fig. 16. With a significant amount of O₂ in the mixture, the AlCl₃ decomposition rate is dramatically increased. However, the addition of high amounts of O₂, in the presence of H₂, is predicted by this kinetic model to lead, under adiabatic conditions, to ignition. In contrast, mixtures 2 and 3 are predicted to react under nearly isothermal and isobaric conditions due to the low level of oxygen present in the mixture. Therefore, this promoting effect of oxygen can be of potential use in the CVD process to reduce the

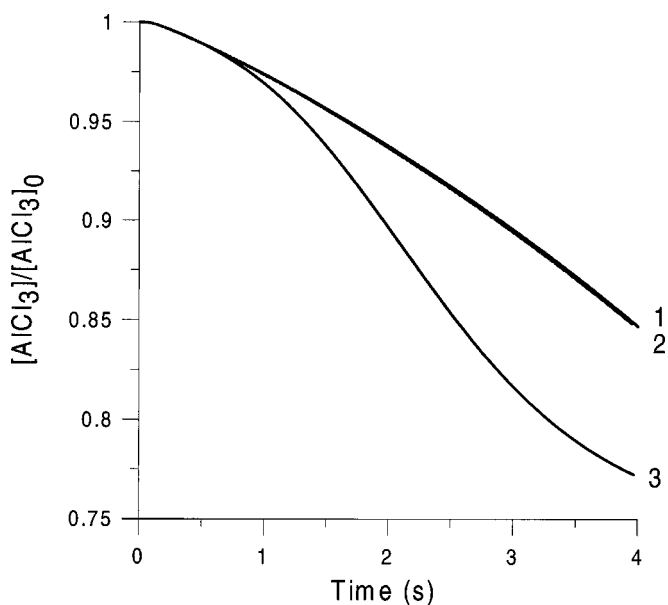


Figure 15. Calculated AlCl₃ profiles at total pressure of 100 mbar and at 1323 K for the mixtures: (1) 0.06 mbar HCl + 1.3 mbar AlCl₃ + 4 mbar CO₂ + 60 mbar H₂ in Ar; (2) H₂, AlCl₃, and CO₂ as in 1 + 0.06 mbar CO in Ar; and (3) H₂, AlCl₃, and CO₂ as in 1 + 26 mbar CO in Ar.

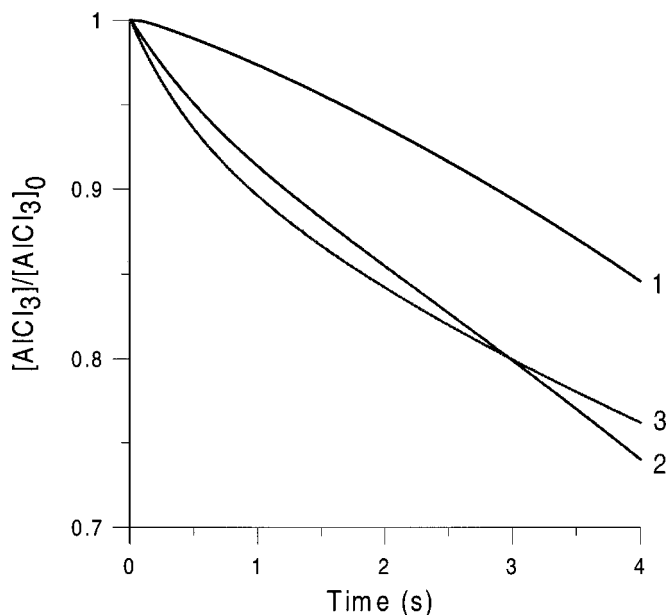


Figure 16. Calculated AlCl_3 profiles at total pressure of 100 mbar and at 1323 K for the mixtures: (1) 0.06 mbar HCl + 1.3 mbar AlCl_3 + 4 mbar CO_2 + 60 mbar H_2 in Ar; (2) H_2 , AlCl_3 , and CO_2 as in 1 + 0.06 mbar O_2 in Ar; and (3) H_2 , AlCl_3 and CO_2 as in 1 + 0.1 mbar O_2 in Ar.

deposition times. However, as underlined above, these kinetics considerations only concern the gas phase, and the predicted promoting effect of molecular oxygen has to be experimentally demonstrated. Again, use of oxygen in this system would introduce potential explosion hazards, and detailed kinetic modeling could be of use in defining these.

Conclusions

A kinetic model has been built to examine the gas-phase chemistry between the precursors AlCl_3 and CO_2 in the presence of H_2 during thermal CVD of alumina. This kinetic model can explain several trends observed experimentally, including the promoting effect of H_2 , the inhibiting effect of HCl , and the effect of temperature not directly on the alumina deposition kinetics, but indirectly on the aluminum precursor decomposition. The AlCl_3 decomposition is predicted to occur via a free-radical chain mechanism that, in the

presence of H_2 , has H atoms and the AlCl_2 radical as the primary chain carriers. Sensitivity analyses have been performed to examine the reaction pathways for the decomposition of the precursor as well as for the formation of water, a molecule that has been proposed to play a major role in the heterogeneous chemistry. Depending on the rate constant taken for the reaction $\text{CO} + \text{OH} \leftrightarrow \text{CO}_2 + \text{H}$, the $\text{CO}_2 + \text{H}_2$ global reaction (water-gas shift) is shown to produce either (i) very little water at the temperatures of interest for the CVD processes, and a reaction sequence is proposed to explain the formation of water in significant amounts, or (ii) to produce water competitively with the other water-producing channels $\text{AlO} + \text{H}_2 \leftrightarrow \text{H}_2\text{O} + \text{Al}$ and $\text{HCl} + \text{OH} \leftrightarrow \text{H}_2\text{O} + \text{Cl}$. The effects of some additives on the AlCl_3 decomposition rate have been examined with the help of the above kinetic model. Cl_2 is predicted to be a more efficient inhibitor than HCl . Water is predicted to have no effect even if high amounts are added. Hydrogen peroxide and molecular oxygen are predicted to be promoters, even at very low levels.

Acknowledgments

This work was partially supported by generous grants of super-computer resources from the University at Buffalo (SUNY) Center for Computational Research.

References

1. B. Lux and H. Schachner, *High Temp.-High Press.*, **10**, 315 (1978).
2. R. Colmet, R. Naslain, P. Hagenmuller, and C. Bernard, *J. Electrochem. Soc.*, **129**, 1367 (1982).
3. C. Colombier, B. Lux, and J. Lindström, *Int. J. Refract. Hard Met.*, **5**, 222 (1986).
4. Y. W. Bae, W. Y. Lee, T. M. Besmann, O. B. Cavin, and T. R. Watkins, *J. Am. Ceram. Soc.*, **81**, 1945 (1998).
5. M. Shierling, E. Zimmermann, and D. Neuschütz, *J. Phys. IV*, **9**, 85 (1999).
6. S. F. Nitodas and S. V. Sotirchos, *J. Electrochem. Soc.*, **147**, 1050 (2000).
7. S. F. Nitodas and S. V. Sotirchos, *Chem. Vap. Deposition*, **5**, 219 (1999).
8. M. T. Swihart, L. Catoire, B. Legrand, I. Gökulp, and C. Paillard, *Combust. Flame*, Submitted.
9. M. T. Swihart and L. Catoire, *J. Phys. Chem. A*, **105**, 264 (2001).
10. R. J. Kee, F. M. Rupley, and J. A. Miller, Report SAND89-8009B.UC-706, Sandia National Laboratories (1991).
11. A. E. Lutz, R. J. Kee, and J. A. Miller, Report SAND87-8248.UC-401, Sandia National Laboratories (1987); A. E. Lutz, R. J. Kee, and J. A. Miller, *Chemkin II Version 3.0 Program*, Sandia National Laboratories (1994).
12. M. T. Swihart and L. Catoire, *Combust. Flame*, **121**, 210 (2000).
13. R. J. Kee, F. M. Rupley, and J. A. Miller, Report SAND87-8215B.UC-4, Sandia National Laboratories (1987).
14. A. Burcat and B. McBride, Report 804, Technion Aerospace Engineering (1997).
15. C. W. Larson, P. H. Stewart, and D. M. Golden, *Int. J. Chem. Kinet.*, **20**, 27 (1988).
16. M. S. Wooldridge, R. K. Hanson, and C. T. Bowman, *Int. J. Chem. Kinet.*, **28**, 361 (1996).